

Numerical Investigation of the Two-Component Suspension Filtration in a Porous Medium Taking into Account Changes in the Characteristics of the Porous Medium

BEKZODJON FAYZIEV¹, JAMOL MAKHMUDOV¹, JABBOR MUSTOFOQULOV²,
TULKIN BEGMATOV¹, RAKHMOM SAFAROV¹

¹Department of Mathematical modeling,
Samarkand State University,
Samarkand, 140100,
UZBEKISTAN

²Department of Radioelectronics,
Jizzakh Polytechnic Institute,
Jizzakh, 140300,
UZBEKISTAN

Abstract: The paper explores a mathematical model of the filtration of dual-component suspension within a porous medium characterized by two distinct zones. This model encompasses mass balance equations of suspended particles, kinetic equations of deposition formation for both reversible and irreversible deposition types for each suspension component, and incorporates Darcy's law. In order to solve the problem, we formulate a numerical algorithm for computer-based experimentation on the basis of the finite difference method. Through the analysis of numerical findings, we establish key features of two component suspension filtration within a porous medium. Furthermore, we examine the effects of model parameters on the transport and deposition of suspended particles in a two-component suspension within porous media. The polydispersity of the suspension and the multi-stage nature of deposition kinetics can induce effects that differ from those typically observed in the transport of one-component suspensions with single-stage particle deposition kinetics.

Key-Words: deep bed filtration, finite difference method, multistage deposition, porous media, mathematical model, two component suspension

Received: December 16, 2022. Revised: October 24, 2023. Accepted: November 19, 2023. Published: December 22, 2023.

1 Introduction

The phenomenon of suspension filtration, including transport and deposition of suspended particles are common occurrences that occur frequently within the wide scope of industrial and natural processes. In groundwater, solid particles may be a specific contaminant, or the particles may carry solutes with it, promoting their movement by transport much faster and longer than normal solute diffusion. Conversely, in some cases, if their aggregates settle in the environment, these particles may solidify and hinder the migration of flocculating agents, [1], [2]. Filtration through porous media is primarily used for the removal of micron-sized particles from aqueous flow in the purification of drinking and wastewater, [3]. In the oil industry, suspended particles in water sent through reservoirs can accumulate in the well, leading to a decrease in productivity, [4]. The release of soil particles during construction can contribute to inter-

nal erosion and subsequent degradation of hydraulic structures, [5], [6].

The majority of actual suspensions exhibit a multi-component nature. The solid particles present in these suspensions can vary in terms of their properties, encompassing differences in geometric, physicochemical, and electrokinetic characteristics, [7], [8]. Recent studies have increasingly taken into account the polydispersity of such suspensions, [9], [10], [11], [12]. Among multi-component suspensions, the simplest form is the two-component suspension, composed of two dispersed components with distinct concentrations and kinetic properties. Consequently, the focus of research has predominantly been on two-component suspensions, [11], [12].

To model the transport and deposition of suspended particles developed different approach, such as, pore-network modeling, [13], [14], particle trajectory analysis models, [15], and empirical models,

[11], [12], [16]. In the network models, a filter is conceptualized as a porous medium comprising interconnected microscopic units. Estimating the time-dependent particle distribution within the filter involves assessing the retained particles in each cell. A significant drawback in the predictability of models for large-scale particulate systems is the considerable limitation posed by low particle injection efficiency, [13], [14]. The initial proposal of the particle trajectory model, alternatively known as the unit bed elements model, can be traced back to [15]. The precision of this model is heavily influenced by the choice of conceptual representations for porous media. Various existing models serve this purpose, encompassing capillaries, spherical structures, constricted tubes, and the capillaries-chambers model [15]. The phenomenological model characterizes the macroscopic filtration process through the formulation of a set of phenomenological equations and the introduction of a range of empirically determined coefficients. Numerous researchers have suggested numerical solutions for the phenomenological model and analytical methods to determine capturing coefficients under diverse mechanisms [11], [12], [17].

In this paper, we use phenomenological approach to formulate a problem of two component suspension filtration in a dual-zone porous medium. Which is described as system of partial differential equations. Therefore, the system of multi-component suspension filtration equations is a generalization of the single-component case, and the mass balance equation for each component of the suspension is ($i = 1, 2$), [12], [18], [19]

$$m_0 \frac{\partial c^{(i)}}{\partial t} + v \frac{\partial c^{(i)}}{\partial x} + \frac{\partial \rho_a^{(i)}}{\partial t} + \frac{\partial \rho_p^{(i)}}{\partial t} = 0, \quad (1)$$

where m_0 is the porosity of the medium, v is the velocity (m/s), $c^{(i)}$ are concentrations of i^{th} component of the suspension (m^3/m^3), $\rho_a^{(i)}$, $\rho_p^{(i)}$ are concentrations of deposition of i^{th} component formed in the active and passive zones, respectively (m^3/m^3), $i = 1, 2$ correspond to the component numbers.

Kinetic equation of reversible deposition formation

$$\frac{\partial \rho_a^{(i)}}{\partial t} = \beta_a^{(i)} \left(c^{(i)} - \frac{\rho_a^{(i)}}{\rho_{a0}^{(i)}} c_0^{(i)} \right) \quad (2)$$

where $\beta_a^{(i)}$ are kinetic coefficients characterizing the intensity of deposition formation in the active zone for the i^{th} component of the suspension, $\rho_{a0}^{(i)}$ are capacities of the active zones for i^{th} component of the suspension.

The equation for the kinetics of irreversible depo-

sition formation:

$$\frac{\partial \rho_p^{(i)}}{\partial t} = \beta_p^{(i)} \phi_i \left(\rho_p^{(1)}, \rho_p^{(2)} \right) c^{(i)}. \quad (3)$$

where $\rho_{p0}^{(i)}$ are partial capacities of passive zones. As in. [19] the total capacitance of passive zone of the filter ρ_{p0} is mainly determined by the first fraction, as well as $\rho_{p0}^{(1)} > \rho_{p0}^{(2)}$. As a result, deposition in the passive zone stops when the sum $\rho_p^{(1)} + \rho_p^{(2)}$ equals the total capacitance ρ_{p0} . In addition, the deposition formation for the second fraction $\rho_p^{(2)}$ stops when the concentration is equal to its partial capacity, although $\rho_p^{(1)} + \rho_p^{(2)} < \rho_{p0}$ the total capacity is not full. Also, the "kinetic properties" of the first fraction are higher, i.e. $\beta_p^{(1)} / \beta_p^{(2)} > 1$.

Parameters $\phi_i \left(\rho_p^{(1)}, \rho_p^{(2)} \right)$ characterizing the "aging" phenomenon are as follows, [19]

$$\phi_1 \left(\rho_p^{(1)}, \rho_p^{(2)} \right) = \begin{cases} 1, & 0 < \rho_p^{(1)} \leq \rho_{p1}^{(1)}, \\ \rho_{p1}^{(1)} / \rho_p^{(1)}, & \rho_{p1}^{(1)} < \rho_p^{(1)}, \\ \rho_p^{(1)} + \rho_p^{(2)} < \rho_{p0}, \\ 0, & \rho_p^{(1)} + \rho_p^{(2)} = \rho_{p0}, \end{cases} \quad (4)$$

$$\phi_2 \left(\rho_p^{(1)}, \rho_p^{(2)} \right) = \begin{cases} 1, & 0 < \rho_p^{(2)} \leq \rho_{p1}^{(2)}, \\ \rho_{p1}^{(2)} / \rho_p^{(2)}, & \rho_{p1}^{(2)} < \rho_p^{(2)} < \rho_{p0}, \\ \rho_p^{(1)} + \rho_p^{(2)} < \rho_{p0}, \\ 0, & \rho_p^{(1)} + \rho_p^{(2)} = \rho_{p0}, \end{cases} \quad (5)$$

where $\rho_{p1}^{(i)}$ are threshold concentrations, $\rho_p^{(i)} > \rho_{p1}^{(i)}$ from which the phenomenon of "aging" begins in the passive zone.

2 Problem Formulation

We consider semi-infinite porous media filled with homogeneous liquid (that is, a liquid without suspended particles) and the initial value of porosity is m_0 . At the point, $x = 0$ from the moment $t > 0$ inhomogeneous liquid containing two different solid particles with concentration $c_0 = c_0^{(1)} + c_0^{(2)}$ is injected into the porous media with the constant velocity v_0 .

In the balance equation (1), the change in the characteristics of the pore medium as a result of deposition was not taken into account. But as mentioned in, [12] deposition significantly change the properties of the porous medium, so we change this equation as follows

$$\frac{\partial (mc^{(i)})}{\partial t} + v \frac{\partial c^{(i)}}{\partial x} + \frac{\partial \rho_a^{(i)}}{\partial t} + \frac{\partial \rho_p^{(i)}}{\partial t} = 0, \quad (6)$$

where m is the current porosity of the medium. It is calculated as follows

$$m = m_0 - \left(\rho_a^{(1)} + \rho_a^{(2)} + \rho_p^{(1)} + \rho_p^{(2)} \right) \quad (7)$$

We use the Carman–Kozeny equation to determine the change in filtration coefficient

$$K(m) = k_0 \frac{m^3}{(1-m)^2}, \quad (8)$$

where $k_0 = \text{const}$ is the filtration coefficient at the initial moment.

The pressure gradient is determined from Darcy's law

$$v = K(m) |\nabla p|. \quad (9)$$

We account for the velocity in both reversible and irreversible deposit formation kinetics, i.e. instead of (2) and (3) we use

$$\frac{\partial \rho_a^{(i)}}{\partial t} = \beta_a^{(i)} v c^{(i)} - \beta_a^{(i)} \frac{\rho_a^{(i)}}{\rho_{a0}^{(i)}} c_0^{(i)} \quad (10)$$

$$\frac{\partial \rho_p^{(i)}}{\partial t} = \beta_p^{(i)} v \phi_i \left(\rho_p^{(1)}, \rho_p^{(2)} \right) c^{(i)}. \quad (11)$$

So, mathematical model of two component suspension filtration consists of equations (4) - (11).

The initial and boundary conditions are as follows:

$$\begin{aligned} c^{(i)}(x, 0) &= 0, \\ \rho_a^{(i)}(x, 0) &= \rho_p^{(i)}(x, 0) = 0, \\ c^{(i)}(0, t) &= c_0^{(i)} = \text{const}. \end{aligned} \quad (12)$$

3 Problem Solution

We use the finite difference method to solve problem (4) - (12), [20], [21]. In the area $D = \{0 \leq x < \infty, 0 \leq t \leq T\}$ we consider following net

$$\begin{aligned} \omega_{h\tau} &= \{(x_k, t_j), x_k = kh, k = 0, 1, \dots, \\ & t_j = j\tau, j = 0, 1, \dots, J, \tau = T/J\}. \end{aligned}$$

Instead of functions $c^{(i)}(t, x)$, $\rho_a^{(i)}(t, x)$, $\rho_p^{(i)}(t, x)$, $m(t, x)$, $\nabla P(t, x)$ functions, (x_k, t_j) we get the net functions $(\rho_a^{(i)})_k^j$, $(\rho_p^{(i)})_k^j$, m_k^j , $|\nabla p|_k^{j+1}$ at the nodes $(c^{(i)})_k^j$.

The balance equation (6) is approximated in the

net for each fraction as follows

$$\begin{aligned} & \frac{m_k^{j+1} (c^{(i)})_k^{j+1} - m_k^j (c^{(i)})_k^j}{\tau} + \\ & v \frac{(c^{(i)})_k^{j+1} - (c^{(i)})_{k-1}^{j+1}}{h} + \frac{(\rho_a^{(i)})_k^{j+1} - (\rho_a^{(i)})_k^j}{\tau} + \\ & \frac{(\rho_p^{(i)})_k^{j+1} - (\rho_p^{(i)})_k^j}{\tau} = 0. \end{aligned} \quad (13)$$

We get the differential scheme for (10) as follows

$$\begin{aligned} & \frac{(\rho_a^{(i)})_k^{j+1} - (\rho_a^{(i)})_k^j}{\tau} = \\ & \beta_a^{(i)} v (c^{(i)})_k^j - \beta_a^{(i)} \frac{(\rho_a^{(i)})_k^j}{\rho_{a0}^{(i)}} c_0^{(i)}. \end{aligned} \quad (14)$$

The non-washable deposition kinetics equation (11) becomes the following after approximation

$$\begin{aligned} & \frac{(\rho_p^{(i)})_k^{j+1} - (\rho_p^{(i)})_k^j}{\tau} = \\ & \beta_p^{(i)} v \phi_i \left((\rho_p^{(1)})_k^j, (\rho_p^{(2)})_k^j \right) (c^{(i)})_k^j. \end{aligned} \quad (15)$$

Schemes (13) - (15) look like this after simple substitutions

$$\begin{aligned} & (c^{(i)})_k^{j+1} = \\ & \left(m_k^j (c^{(i)})_k^j + \frac{\tau v}{h} (c^{(i)})_{k-1}^{j+1} - \right. \\ & \left. (\rho_a^{(i)})_k^{j+1} + (\rho_a^{(i)})_k^j - (\rho_p^{(i)})_k^{j+1} + (\rho_p^{(i)})_k^j \right) \cdot \\ & \left(m_k^{j+1} + \frac{\tau v}{h} \right)^{-1} \end{aligned} \quad (16)$$

$$k = \overline{1, I}, j = \overline{0, J-1},$$

$$\begin{aligned} & (\rho_a^{(i)})_k^{j+1} = \\ & (\rho_a^{(i)})_k^j + \tau \beta_a^{(i)} \left(v (c^{(i)})_k^j - \frac{(\rho_a^{(i)})_k^j}{\rho_{a0}^{(i)}} c_0^{(i)} \right), \end{aligned} \quad (17)$$

$$k = \overline{0, I}, j = \overline{0, J-1},$$

$$\begin{aligned} & (\rho_p^{(i)})_k^{j+1} = (\rho_p^{(i)})_k^j + \\ & \tau \beta_p^{(i)} v \phi_i \left((\rho_p^{(1)})_k^j, (\rho_p^{(2)})_k^j \right) (c^{(i)})_k^j, \end{aligned} \quad (18)$$

$$k = \overline{0, I}, j = \overline{0, J-1}.$$

For equations (7) and (9) we have

$$m_k^{j+1} = m_k^j - \left((\rho_a^{(1)})_k^j + (\rho_a^{(2)})_k^j + (\rho_p^{(1)})_k^j + (\rho_p^{(2)})_k^j \right) \quad (19)$$

$$|\nabla p|_k^{j+1} = \frac{v (1 - m_k^{j+1})^2}{k_0 (m_0 - m_k^{j+1})^3}, \quad (20)$$

Initial and boundary conditions (12) are also approximated on the net $\omega_{h\tau}$

$$\begin{aligned} (\rho_a^{(i)})_k^j &= 0, k = \overline{0, K}, j = 0, \\ (\rho_p^{(i)})_k^j &= 0, k = \overline{0, K}, j = 0, \\ (c^{(i)})_k^j &= 0, k = \overline{0, K}, j = 0, \\ (c^{(i)})_k^j &= c_0^{(i)}, k = 0, j = \overline{0, J}, \end{aligned} \quad (21)$$

Calculations are carried out in the following sequence: from relations (10) and (9) the values of $(\rho_n^{(i)})_k^{j+1}$, $(\rho_n^{(i)})_k^j$ and $(\rho_a^{(i)})_k^j$ are $(\rho_a^{(i)})_k^{j+1}$ found based on the values of $(c^{(i)})_k^{j+1}$ and at the corresponding points in the lower layer, then from (8) $(c^{(i)})_k^j$.

4 Results and discussion

We take the following numerical values of the parameters as initial values: $c_0^{(1)} = 0.05$, $c_0^{(2)} = 0.03$, $m_0 = 0.3$, $v = 10^{-4} \text{ m/s}$, $\rho_0 = 0.1$, $\rho_{a0} = 0.01$, $\rho_{a0}^{(1)} = 0.007$, $\rho_{a0}^{(2)} = 0.003$, $\rho_{p0} = 0.09$, $\rho_{p0}^{(1)} = 0.06$, $\rho_{p0}^{(2)} = 0.03$, $\beta_{a0}^{(1)} = 50 \text{ s}^{-1}$, $\beta_{a0}^{(2)} = 30 \text{ s}^{-1}$, $\beta_{p0}^{(1)} = 50 \text{ s}^{-1}$, $\beta_{p0}^{(2)} = 30 \text{ s}^{-1}$.

Let's go to the analysis of the results. At the certain points of the porous media the values of $c^{(i)}$, $\rho_a^{(i)}$ and $\rho_p^{(i)}$ increase over time (Fig.1, Fig.2). As passive zone capacities the values $\rho_{p0}^{(1)} = 0.06$, $\rho_{p0}^{(2)} = 0.03$ are taken. As can be seen from Figure 1. b, the concentration of the first component near the point $x = 0$ exceeds the capacity of the passive zone for this fraction, i.e. $\rho_p^{(1)} > \rho_{p0}^{(1)}$. This shows that the capacity of the passive zone for the second fraction is filled not only with concentration $\rho_p^{(2)}$, but also with $\rho_p^{(1)}$. At about $t > 900 \text{ s}$, the concentration of the second fraction increases to some extent x and then decreases.

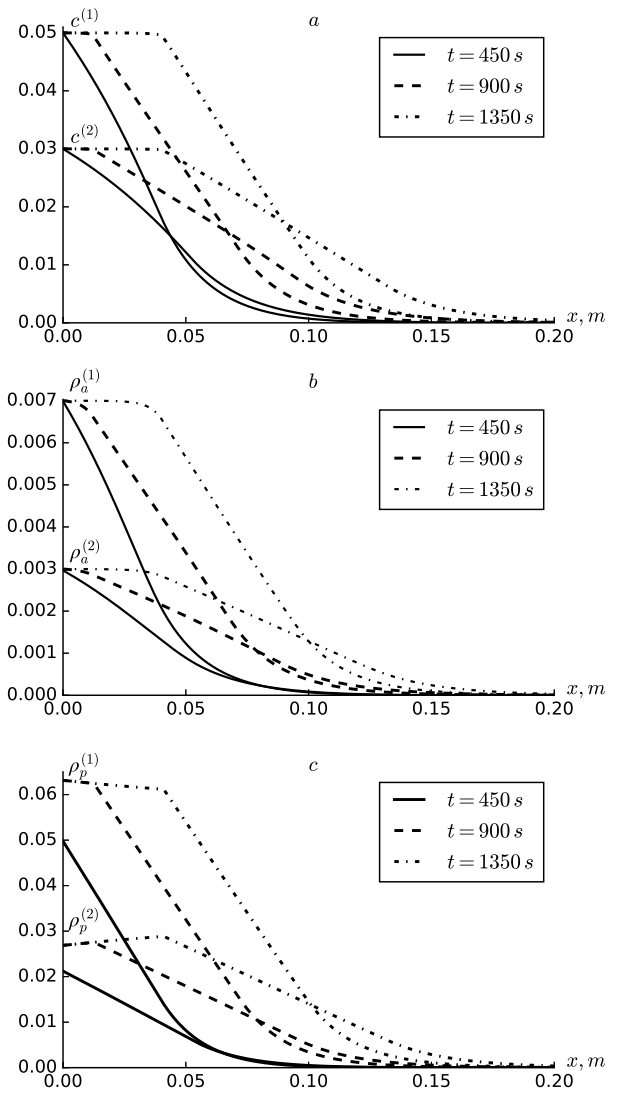


Figure 1: Profiles of $c^{(1)}$, $c^{(2)}$ (a), $\rho_a^{(1)}$, $\rho_a^{(2)}$ (b), $\rho_p^{(1)}$, $\rho_p^{(2)}$ (c) at $\rho_{p1}^{(1)} = 0.015$, $\rho_{p1}^{(2)} = 0.006$.

Over time the coordinate of the increment of $\rho_p^{(2)}$ becomes larger. If the value of the parameters $\rho_{p1}^{(1)}$ and $\rho_{p1}^{(2)}$ are increased, from $t \geq 450$ in the points close to the point $x = 0$, the capacity of the passive zone ρ_{p0} is completely saturated with deposition (Fig. 2). From Fig. 1.a. can be seen that at $t \leq 450 \text{ s}$ concentrations of suspended particles for both types are reached their maximum value only at inlet point, but from $t \geq 950 \text{ s}$ the maximum value has been reached at points $x \leq 0.01 \text{ m}$, and at $t = 1350 \text{ s}$ almost till to $x \leq 0.05 \text{ m}$. Comparing figures Fig. 1.a. and Fig. 2.a. one can see that increasing the parameters $\rho_{p1}^{(1)}$ and $\rho_{p1}^{(2)}$ leads to further reaching the maximum concentrations.

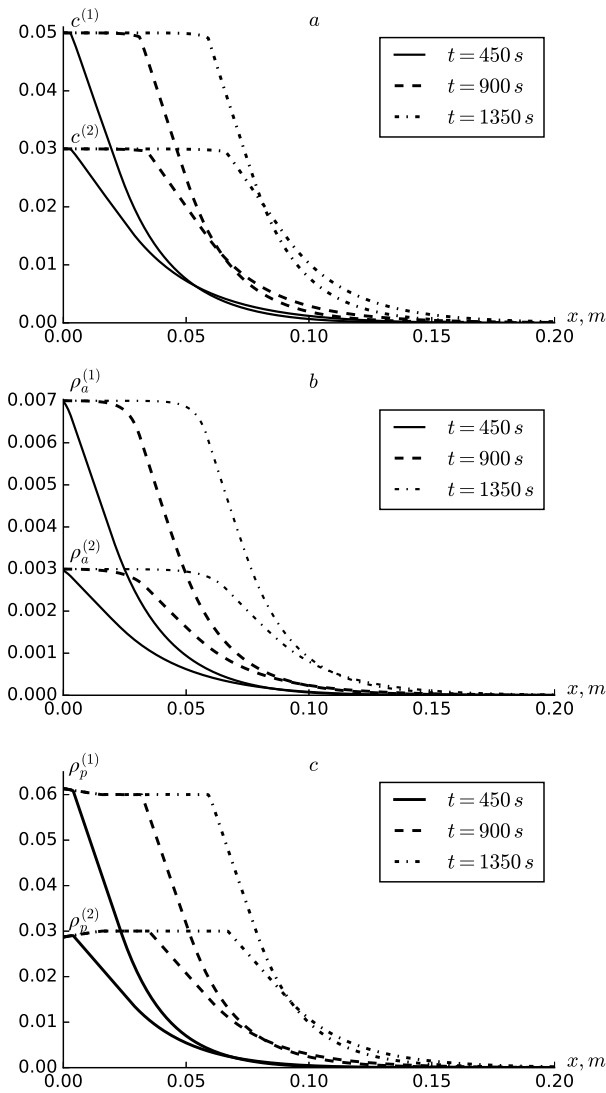


Figure 2: Profiles of $c^{(1)}$, $c^{(2)}$ (a), $\rho_a^{(1)}$, $\rho_a^{(2)}$ (b), $\rho_p^{(1)}$, $\rho_p^{(2)}$ (c) at $\rho_{p1}^{(1)} = 0.03$, $\rho_{p1}^{(2)} = 0.015$.

Figure 3 shows the changing dynamics of $\rho_p^{(i)}$ for different values of $\rho_{p1}^{(i)}$. It can be seen from the graphs an increase in the values of $\rho_{p1}^{(i)}$ leads to an increase in the intensity of deposition formation in the passive zone at the initial values of time. In the case of less values of $\rho_{p1}^{(i)}$ it takes less time to reach maximum value of $\rho_p^{(i)}$. At the point $x = 0$ the maximum values of $\rho_p^{(i)}$ reached at approximately 400 and 700 s (Fig.3.a.), however at the point $x = 0.03$ at takes approximately 800 and 1200 s, respectively (Fig.3.b.).

At a fixed value of $\rho_{p1}^{(i)}$ the change profiles of $|\nabla P|$, m at different times are shown in Figure 4. On the whole, an increase can be observed for $|\nabla P|$,

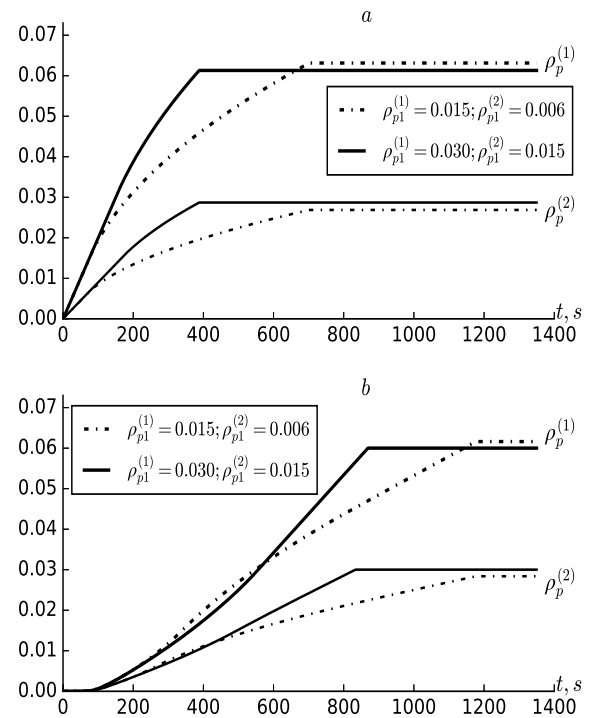


Figure 3: Dynamics of $\rho_p^{(1)}$ and $\rho_p^{(2)}$ at the points $x = 0$ m (a) and $x = 0.03$ m (b), at different values of $\rho_{p1}^{(i)}$.

and a decrease for m . As it can be seen from (7), due to the formation of deposition of particles in the active and passive zones of the medium (which means the increase of $\rho_a^{(i)}$ and $\rho_p^{(i)}$), the active porosity of the medium decreases. As it can be seen from (8), decreasing the value of current porosity m leads to a decrease in the filtration coefficient $K(m)$ according to the Carman-Kozeny law, because the both decreasing the value of numerator of fraction and increasing the value of denominator of fraction leads to decreasing the value of fraction. Since we are considering a regime with a constant filtration rate the pressure gradient $|\nabla P|$ at different points in this medium leads to an increase. The increasing character of $|\nabla P|$ of can be seen in Fig. 4a, and the decreasing character of m in Fig. 4b.

5 Conclusion

Model of filtration of two-component suspensions in porous media improved including changes in the characteristics of the porous media, dynamic factors, multi-stage deposition formation and diffusion. In this work the changes of characteristics of porous media (porosity, permeability) are taken into account directly in the model. It lead to analyse the role of different types deposition formation in filtration process.

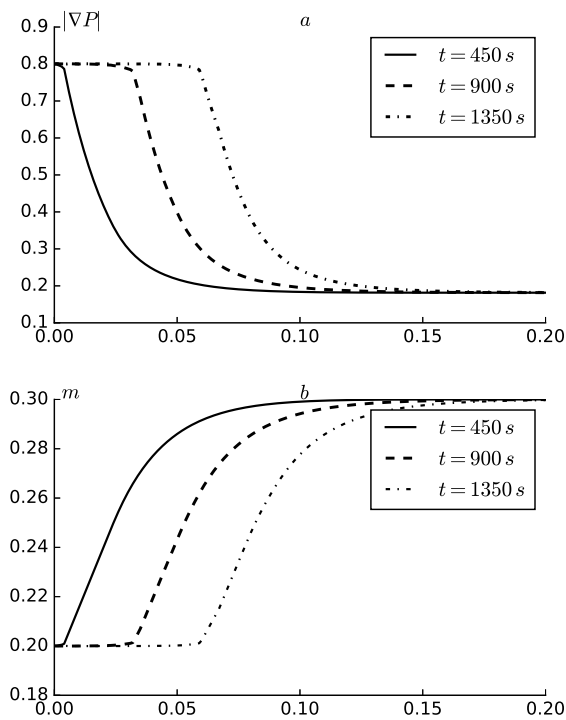


Figure 4: Profiles of $|\nabla P|$ (a) and m (b) at $\rho_{p1}^{(1)} = 0.03$, $\rho_{p1}^{(2)} = 0.015$.

An effective algorithm has been developed on the basis of finite difference method. It is shown that taking into account the multi-stage nature of deposition formation leads to situations that are not observed in single-step kinetics. In particular, non-monotonicity was observed in the dynamics of deposition formation at certain points.

The authors need to clarify and explain the difference between the current study with the available literature, as well as the main contribution of the study in order to emphasize the main research outcomes of the paper.

The unique aspect of filtering two-component suspensions in porous media lies in the possibility of the deposition of first component within the passive zone, surpassing the environmental capacity designated for it. This scenario arises as the deposition of the first component intensifies, not solely due to the presence of the second component, but also because the capacity reserved for the second component can be partially occupied by the first component.

In the future works this model will be improved for n component suspension filtration. Also it will be better to conduct laboratory experiments to estimate the adequateness of the developed mathematical model.

References:

- [1] Kanti Sen, T., Kartic, C.K., Review on sub-surface colloids and colloid-associated contaminant transport in saturated porous media, *Advances in Colloid and Interface Science*, Vol. 119, No. 2-3, 2006, pp. 71–96. <https://doi.org/10.1016/j.cis.2005.09.001>.
- [2] Aim, R.B., Vigneswaran, S., Prasanthi, H., Jegatheesan, V., Influence of Particle Size and Size Distribution in Granular Bed Filtration and Dynamic Microfiltration, *Water Science and Technology*, Vol. 36, No. 4, 2013, pp. 56–65. <https://doi.org/10.1016/j.colsurfa.2012.10.018>
- [3] Sadiq, R., Husain, T., Al-Zahrani, A.M., Sheikh, A.K., Farooq, S., Secondary effluent treatment by slow sand filters: performance and risk analysis. *Water Air Soil Pollut*, Vol. 143, 2003, pp. 41–63. <https://doi.org/10.1023/A:1022894531638>
- [4] Feia S.,J-C. Dupla, J. Sulem, S. Ghabezloo, J. Canou, A. Onaisi, H. L., Transport and deposition of solid particles in uncemented petroleum reservoirs. *21st French Congress of Mechanics.*, 2013.
- [5] Khuzhaerov, B., Effects of blockage and erosion on the filtration of suspensions. *Journal of Engineering Physics*, Vol. 58, 1990, pp. 185–190. <https://doi.org/10.1007/BF00872845>
- [6] Al-Fares, W., Contribution of the geophysical methods in characterizing the water leakage in Afamia B dam, Syria. *Journal of Applied Geophysics*, Vol. 75, No. 3, 2011, pp. 464–471. <https://doi.org/10.1016/j.jappgeo.2011.07.014>
- [7] Tien C., Ramarao B.V., *Granular Filtration of Aerosols and Hydrosols 2nd ed*, Elsevier, Amsterdam, 2007.
- [8] Elimelech M., Gregory J., Jia X., Williams R.A., *Particle Deposition and Aggregation: Measurement, Modelling, and Simulation. Colloid and Surface Engineering Series*, Butterworth-Heinemann, Oxford, 1989.
- [9] Khuzhayorov B., A model of multicomponent grouting and suffosion filtration, *Journal of Engineering Physics and Thermophysics*, Vol. 66, 1994, pp. 373-379; doi:10.1007/BF00853459.
- [10] Khuzhayorov B., Model of colmatage-suffosion filtration of disperse systems in a porous medium, *Journal of Engineering Physics and Thermophysics*, Vol. 73, 2000, pp. 668-673; doi:10.1007/s10891-000-0073-x

- [11] Hammadi A. , Ahfir N.D., Alem A. , Wang H., Effects of particle size non-uniformity on transport and retention in saturated porous media, *Transport in Porous Media*, Vol. 118, 2017, pp. 1-14. doi:10.1007/s11242-017-0848-6.
- [12] Khuzhayorov, B.; Fayziev, B.; Ibragimov, G.; Md Arifin, N. A Deep Bed Filtration Model of Two-Component Suspension in Dual-Zone Porous Medium. *Appl. Sci.*, Vol. 10, 2020, 2793. <https://doi.org/10.3390/app10082793>
- [13] Yang, H.T., Balhoff, M.T. Pore-network modeling of particle retention in porous media. *AIChE Journal* , Vol. 63, 2017, pp. 3118–3131.
- [14] Minhui Qi, Mingzhong Li, Rouzbeh G. Moghanloo, Tiankui Guo, A novel simulation approach for particulate flows during filtration, Vol. 67, No. 4, (2021). *AIChE Journal* , Vol. 67, No. 4. 2021, e17136.
- [15] Payatakes A, Rajagopalan R, Tien C. Application of porous media models to the study of deep bed filtration, *The Canadian Journal of Chemical Engineering*, Vol. 52, No. 6, 1974, pp. 722-731.
- [16] Khuzhayorov, B. Kh., Makhmudov J. M. Flow of Suspensions in Two-Dimensional Porous Media with Mobile and Immobile Liquid Zones, *Journal of Porous Media*, Vol. 13, No. 5, 2010, pp. 423–37. <https://doi.org/10.1615/jpormedia.v13.i5.30>.
- [17] Chequer L., Bedrikovetsky P. Suspension-colloidal flow accompanied by detachment of oversaturated and undersaturated fines in porous media, *Chemical Engineering Science*, Vol. 198, 2019, pp. 16-32.
- [18] Venetsianov E.V., Rubinshtein R., *Dynamic of Sorption from Liquid Media* Nauka. Moscow, 1983 [in Russian].
- [19] Gitis V., Rubinstein, I., Livshits, M., Ziskind, G. Deep-bed filtration model with multistage deposition kinetics, *Chemical Engineering Journal*, Vol. 163, No 1-2, 2010, pp. 78-85; doi: 10.1016/j.cej.2010.07.044.
- [20] Bekzodjon Fayziev, A phenomenological model of suspension filtration in porous medium, *International Journal of Applied Mathematics*, Vol. 33, No. 3, 2020, pp. 511-521. doi: <http://dx.doi.org/10.12732/ijam.v33i3.10>
- [21] Samarskii, A.A. *The Theory of Difference Schemes*; CRC Press: New York, NY, USA, 2001.

Contribution of Individual Authors to the Creation of a Scientific Article (Ghostwriting Policy)

The authors equally contributed in the present research, at all stages from the formulation of the problem to the final findings and solution.

Sources of Funding for Research Presented in a Scientific Article or Scientific Article Itself

No funding was received for conducting this study.

Conflicts of Interest

The authors have no conflicts of interest to declare that are relevant to the content of this article.

Creative Commons Attribution License 4.0 (Attribution 4.0 International , CC BY 4.0)

This article is published under the terms of the Creative Commons Attribution License 4.0 https://creativecommons.org/licenses/by/4.0/deed.en_US